nature medicine

ARTICLES

# A primate-specific, brain isoform of *KCNH2* affects cortical physiology, cognition, neuronal repolarization and risk of schizophrenia

Stephen J Huffaker[1,2], Jingshan Chen[1,2], Kristin K Nicodemus[1,2], Fabio Sambataro[1,2], Feng Yang[3], Venkata Mattay[1,2], Barbara K Lipska[1,2], Thomas M Hyde[1,2], Jian Song[1,2], Dan Rujescu[4], Ina Giegling[4], Karine Mayilyan[5], Morgan J Proust[1], Armen Soghoyan[5], Grazia Caforio[6], Joseph H Callicott[1], Alessandro Bertolino[6], Andreas Meyer-Lindenberg[1,2,7], Jay Chang[2,3], Yuanyuan Ji[3], Michael F Egan[1], Terry E Goldberg[1,2], Joel E Kleinman[1,2], Bai Lu[2,3] & Daniel R Weinberger[1,2]



**Organized neuronal firing is crucial for cortical processing and is disrupted in schizophrenia. Using rapid amplification of 5′ complementary DNA ends in human brain, we identified a primate-specific isoform (3.1) of the ether-a-go-go–related $K^+$ channel *KCNH2* that modulates neuronal firing. *KCNH2*-3.1 messenger RNA levels are comparable to full-length *KCNH2* (1A) levels in brain but three orders of magnitude lower in heart. In hippocampus from individuals with schizophrenia, *KCNH2*-3.1 expression is 2.5-fold greater than *KCNH2*-1A expression. A meta-analysis of five clinical data sets (367 families, 1,158 unrelated cases and 1,704 controls) shows association of single nucleotide polymorphisms in *KCNH2* with schizophrenia. Risk-associated alleles predict lower intelligence quotient scores and speed of cognitive processing, altered memory-linked functional magnetic resonance imaging signals and increased *KCNH2-3.1* mRNA levels in postmortem hippocampus. KCNH2-3.1 lacks a domain that is crucial for slow channel deactivation. Overexpression of *KCNH2-3.1* in primary cortical neurons induces a rapidly deactivating $K^+$ current and a high-frequency, nonadapting firing pattern. These results identify a previously undescribed KCNH2 channel isoform involved in cortical physiology, cognition and psychosis, providing a potential new therapeutic drug target.**

A major challenge in modern medicine is to understand cellular and molecular mechanisms underlying common mental illnesses such as schizophrenia, which involve complicated genetic and environmental determinants[1]. Prevailing etiological hypotheses maintain that the interaction of multiple genetic factors with each other and with environmental risk factors results in neurodevelopmental abnormalities predisposing to illness later in life[1]. Given this complexity, together with imprecise and differing definitions of phenotype, it is not surprising that statistical association studies to identify risk genes for schizophrenia have not been easily reproduced[1,2]. Gene identification for complex polygenic disorders such as schizophrenia will probably require demonstration that risk variants affect the biology of the gene in a manner that converges on key aspects of the biology of the illness[3]. Indeed, this approach has proven to be crucial in a number of complex genetic disorders, such as adult onset diabetes, in which multiple genes each account for only a very small share of risk but show stronger effects on related intermediate phenotypes even in normal individuals, for example, body mass index[4] or glucose-induced insulin release[5]. Potential biological intermediate phenotypes related to risk for schizophrenia include abnormalities related to hippocampal formation and prefrontal cortices, which are consistently reported in patients with schizophrenia and in their healthy relatives[6–11]. Thus, it follows that genes weakly associated with susceptibility for schizophrenia might show relatively robust effects on prefrontal cortex and hippocampal formation function in risk allele–carrying populations.

Here we identify a previously undescribed potential schizophrenia susceptibility gene, *KCNH2* (a human ether-a-go-go (ERG)-family potassium channel), by meta-analyses of five independent clinical association data sets. Moving beyond statistical association with clinical diagnosis, we describe its association with several schizophrenia-linked biological intermediate phenotypes in large samples of normal individuals who carry risk-associated alleles. In searching for a molecular mechanism, we discovered a previously undescribed primate- and brain-specific *KCNH2* isoform (3.1), encoded in close proximity to the risk-associated single nucleotide polymorphisms (SNPs). Expression of *KCNH2*-3.1 is specifically increased within

[1]Clinical Brain Disorders Branch, National Institute of Mental Health (NIMH), Bethesda, Maryland, USA. [2]Genes, Cognition and Psychosis Program, NIMH, Bethesda, Maryland, USA. [3]Section on Neural Development and Plasticity, National Institute of Child Health and Development, Bethesda, Maryland, USA. [4]Molecular and Clinical Neurobiology, Department of Psychiatry, Ludwig Maximilians University, Munich, Germany. [5]Department of Psychiatry and Medical Psychology, Yerevan State Medical University, Health Ministry of Armenian, Yerevan, Armenia. [6]Psychiatric Neuroscience Group, Section on Mental Disorders, Department of Neurological and Psychiatric Sciences, University of Bari, Bari, Italy. [7]Current address: Central Institute of Mental Health, University of Heidelberg/Medical Faculty Mannheim, Germany. Correspondence should be addressed to D.R.W. (weinberd@mail.nih.gov).

Received 21 May 2008; accepted 6 April 2009; published online 3 May 2009; doi:10.1038/nm.1962

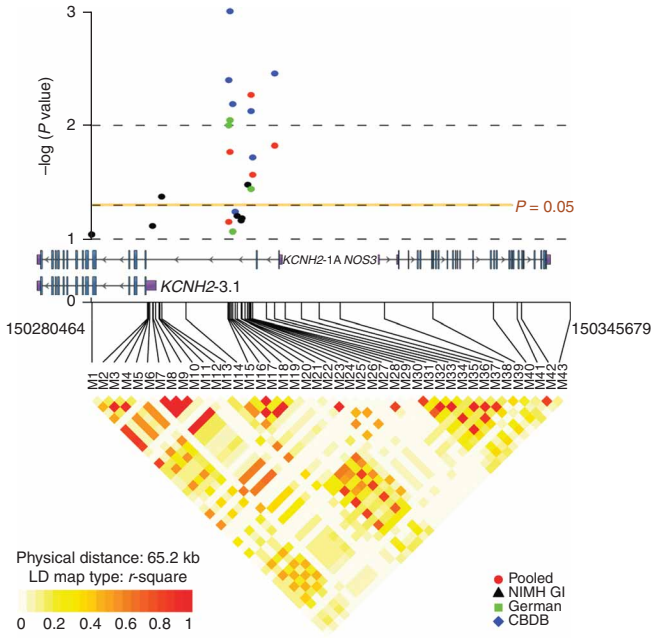


**Figure 1** Genetic association of 7q36.1 with risk for schizophrenia. Top, inverse log of the *P* value for single SNPs from association results for the CBDB/NIMH Sibling Study (blue), for the NIMHGI study (black), for the German case-control study (green) and for the pooled five–data set meta-analysis (Pooled, red). Only markers with *P* values less than 0.1 are shown. A physical map of the region is given and depicts known genes within the region. Bottom, the linkage disequilibrium structure of the genotyped markers for 370 unrelated healthy control subjects of European descent and depicted as $r^2$. Graphic created with the R package snp.plotter[57].

the hippocampal formation of individuals with schizophrenia and in normal individuals who carry risk-associated alleles. Expression of *KCNH2*-3.1 in rodent cortical neurons causes a marked alteration in KCNH2 channel physiology resulting in high-frequency, nonadapting neuronal firing patterns. Such changes in spike frequency may underlie abnormalities in neuronal firing thought to be a fundamental aspect of cortical dysfunction in psychosis[12]. These convergent results implicate KCNH2 in primate cortical physiology and in the etiology and pathophysiology of psychosis, making it a potentially new target for antipsychotic therapy.

## RESULTS

### Identification of *KCNH2* association with schizophrenia

It has become increasingly apparent that genetic risk for schizophrenia and many other complicated illnesses are not related to major amino acid changes or highly detrimental protein mutations, although these may still occur in rare forms of the illness[13]. Instead, the molecular effects of susceptibility alleles are more likely to be subtle, relating to the regulation and splicing of transcripts or proteins. Thus, the gene expression profiles of tissue from individuals with the disease are a potentially informative starting point to search for candidate risk genes[14,15]. We selected ten genes previously reported as differentially expressed in schizophrenic brain[16] and genotyped haplotype-tagging SNPs in 170 families of European descent having an offspring with schizophrenia. Family-based association test (FBAT) analysis[17] of gene-based haplotypes showed significant global association with the genomic region of nitric oxide synthase-3 (*NOS3*; 7q36.1; $P < 0.005$ and $P < 0.05$ after Bonferroni correction for ten association tests) with the diagnosis of schizophrenia (**Supplementary Table 1** online). In the European sample (CEU) of the HapMap Project[18], the block tagged by these SNPs spans portions of *NOS3* and *KCNH2* (**Fig. 1** and **Supplementary Data 1** online). The SNP in this 7q36.1 region that was most strongly associated with schizophrenia is within *KCNH2* and was still associated with the disease after correction for the total number of SNP tests performed across all ten genes (rs1036145, corrected $P = 0.042$, **Supplementary Table 1**).

### *KCNH2* as a potential risk gene for schizophrenia

We genotyped additional SNPs (43 in total) in an expanded sample of 296 families (Clinical Brain Disorders Branch (CBDB) family sample) from the 3′ end of *KCNH2* to the 3′ end of *NOS3*, including 11 SNPs detected through resequencing of the region in individuals with schizophrenia. Six SNPs were significantly associated with schizophrenia at $\alpha < 0.05$ (five with $P < 0.01$; **Fig. 1** and **Supplementary Data 1** and **2** online). Most of the associated markers are in moderate to strong linkage disequilibrium, suggesting the region of interest maps to a ~3-kilobase (kb) of intron 2 of *KCNH2* (**Supplementary Data 1**).

We tested for replication of association in a large German case-control data set, typing the six schizophrenia-associated SNPs found in the CBDB sample and one SNP with marginal significance ($P = 0.057$). We observed significant association at the genotype level for minor-allele homozygotes at four of these SNPs, M16, M17, M19 and M30 (**Fig. 1** and **Supplementary Data 2**). We tested three additional samples with the same six markers: a family–based sample of European ancestry from the US NIMH Genetics Initiative project (NIMHGI)[19], a case-control sample from Armenia and a case-control sample from Italy. Although the sizes and ascertainment strategies differed from those of the larger original samples, in these samples we observed significant association of SNPs in this region with schizophrenia and/or the six implicated SNPs tended toward the same direction of association, although not significantly (**Fig. 1** and **Supplementary Data 2**).

Given these results and power limitations, we conducted a combined family-based and case-control meta-analysis with the R package case-control and transmission disequilibrium test meta-analysis package (Catmap)[20]. This meta-analysis showed SNPs M17, M30, M31 and M33 to be significantly associated with schizophrenia, with M30 showing the greatest odds ratio (1.17) across all samples ($P = 0.0054$; **Supplementary Data 2**). 'Leave-one-out' sensitivity analysis to determine whether the meta-analysis results were driven by the initial family-based result and therefore suggestive of a 'winner's curse' phenomenon[21] revealed that removal of any of the included studies still led to significant association of *KCNH2* with schizophrenia using the four remaining independent studies for SNP M30 (**Supplementary Data 2**). The odds ratios in the cumulative analysis are comparable with other genes reported as significantly associated with schizophrenia in larger meta-analyses[22,23] and exceed the Venice interim criteria for 'small summary' findings[24]. Taken together, these results identify a small intronic region of *KCNH2* as a potential susceptibility locus for schizophrenia.

### Effect of *KCNH2* on cognition and cortical structure and function

Given the high expression of *KCNH2* within the prefrontal cortex and hippocampal formation[25], two brain regions subserving attention and memory processes and consistently implicated in the neuropathology of schizophrenia[26,27], we hypothesized that if risk-associated SNPs affect the biology of these brain regions, cognitive deficits referable to these regions would also be associated with risk genotypes, regardless of disease status. We selected three of the significantly associated SNPs

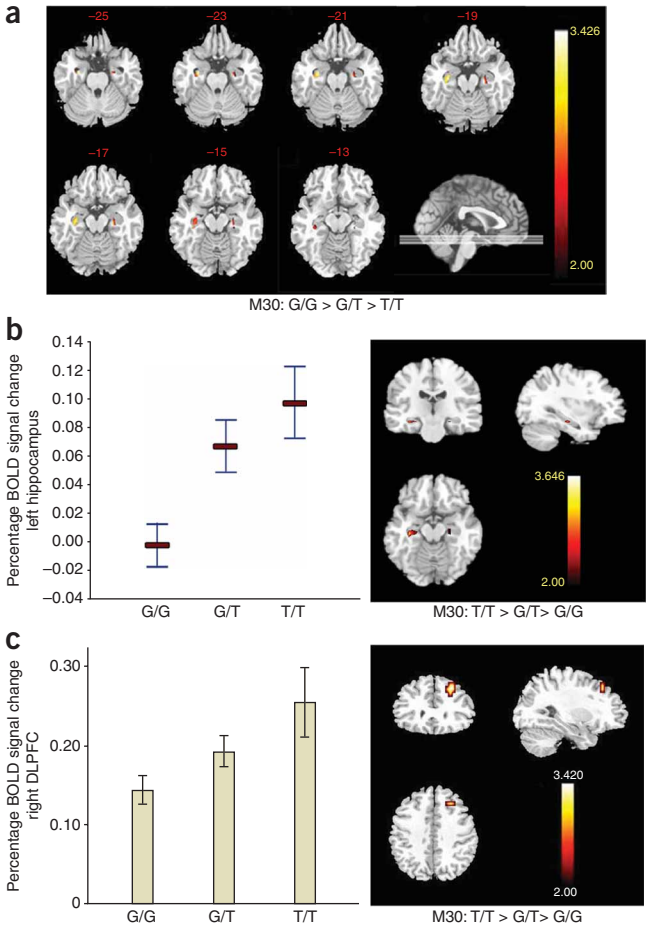


**Figure 2** Association of risk SNPs with cognitive measures, brain structure volumes and regional brain activity during memory-based tasks. (**a**) M30 genotype versus hippocampal gray matter volume in healthy control subjects. Heatmap depicts statistical *t* values of linear decrease in regional gray matter volume from subjects homozygous for the risk associated allele, T, ($n = 16$) to heterozygote carriers ($n = 61$) to noncarriers ($n = 64$). Only voxels corresponding to a $P < 0.05$ FDR corrected threshold are shown. (**b**) Percentage blood oxygen level-dependent (BOLD) signal change in healthy controls during the encoding conditions of a declarative memory task in the left posterior hippocampus (Montreal Neurological Institue (MNI) coordinates of peak cluster: –34 mm, –25 mm and –15 mm) showing a significant ($P = 0.0003$) linear increase of activation of the risk associated allele at M30 in homozygote carriers ($n = 14$) relative to heterozygote carriers ($n = 37$) and to noncarriers ($n = 28$). Plot depicts voxel mean ± s.e.m. Heatmap colors correspond to statistical *t* values of the degree of increase in BOLD signal with each copy of M30 risk allele (T). Only voxels surviving $P < 0.05$ FWE correction are shown. (**c**) Thresholded ($P < 0.05$ FWE corrected) statistical t-maps and mean ± s.e.m. percentage BOLD signal change during the executive working memory task in the right DLPFC (MNI coordinates of peak cluster: 26 mm, 30 mm and 42 mm) showing a significant ($P < 0.005$) linear increase of activation of the risk associated allele at M30 in homozygote carriers ($n = 24$) relative to heterozygote carriers ($n = 71$) and to noncarriers ($n = 81$).

from the meta-analysis (M30, M31 and M33, all of which are in strong linkage disequilibrium with the fourth positively associated SNP, M17) to test for their effects on seven independent summary measures of cognition[28] (**Supplementary Data 3** online) in a sample of healthy, unrelated controls independent from the previous control samples. The use of healthy controls for genetic association at the level of brain function avoids potential confounders related to chronic illness and medical treatment[29]. We observed significant association between risk genotypes for each SNP and performance on the intelligence quotient (IQ) and processing speed factor ($P = 0.020$; **Supplementary Data 3**). Thus, even in healthy controls, the same alleles observed more frequently in individuals with schizophrenia predict significantly lower IQ and processing speed. It is noteworthy that similar cognitive phenotypes have been especially strongly related to genetic risk for schizophrenia in discordant twin samples[7].

We also tested whether the same three SNPs would relate to changes in brain structure and physiology. By magnetic resonance imaging (MRI)-based morphometry, we observed significant volume decreases in hippocampal formation structures ($\alpha = 0.05$, false discovery rate (FDR) corrected), proportional to allelic load, in normal individuals carrying risk alleles of SNPs M30, M31 and M33 using whole-brain and region of interest analyses (**Fig. 2a** and **Supplementary Data 4** online). We next tested whether the same SNPs would influence the physiology of cognitive processing related to hippocampal formation, again in healthy control carriers of risk alleles at SNPs M30, M31 and M33. We used functional MRI (fMRI) to assess regional activation during incidental encoding of a temporal lobe memory task[30] in which task performance was controlled (see **Supplementary Data 4** online for demographic statistics). We observed greater activation (Familywise error (FWE) correction $\alpha = 0.05$) of the hippocampal formation within healthy control risk allele carriers (**Fig. 2b** and **Supplementary Data 4**). This pattern of inefficient processing of memory information (that is, excessive activity for a fixed level of performance) suggests that the tuning of cortical microcircuits crucial for information processing within the hippocampal formation is relatively disordered in individuals with risk-associated alleles. Similar patterns of inefficient processing in hippocampal formation have been reported for other genes and diseases affecting cognition, for example[31,32].

Although hippocampus may be engaged during executive cognition tasks that affect measures of IQ[6,33], recent studies have shown that general intelligence or IQ measures are more closely associated with executive control processes and prefrontal cortex–related structures[34–36]. Therefore, to more specifically investigate a connection between risk-associated alleles and executive-linked physiology, we used fMRI to measure cortical engagement during the N-back working memory task, an executive cognition task well validated as engaging prefrontal cortical circuitry[37]. Again, normal subjects carrying risk-associated alleles of SNPs M30, M31 and M33 showed significantly increased activity in an allele load pattern within the dorsolateral prefrontal cortex (DLPFC), despite controlled task performance (that is, inefficient cortical processing; **Fig. 2c** and **Supplementary Data 4**). In conjunction with significantly increased hippocampal formation activity during memory-encoding tasks, again in normal subjects, these data consistently suggest association between risk alleles and impairments in the efficiency of information processing within two areas of the brain implicated in the pathophysiology of schizophrenia.

## Risk genotypes and *KCNH2* mRNA levels

The association of *KCNH2* with schizophrenia and with related brain phenotypes in multiple independent samples lends statistical and biological support to the involvement of this genomic region in risk of illness. However, these findings do not identify the underlying molecular mechanism. We investigated gene expression in human brain and its relationship to our evidence for genetic association

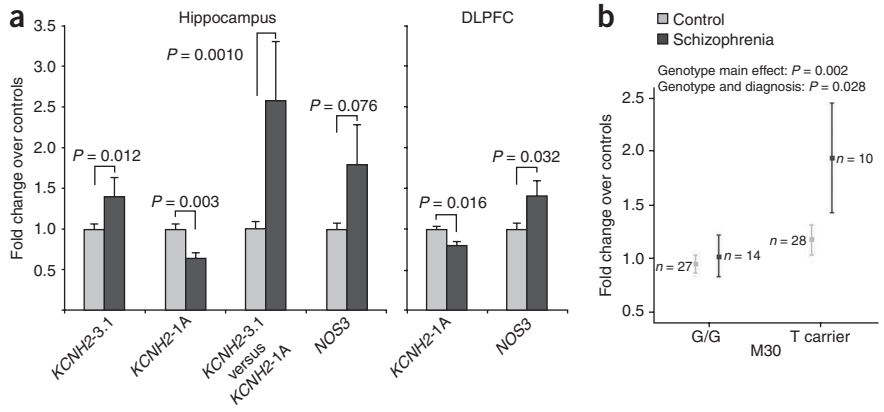


**Figure 3** Regional gene expression and association with risk genotype. (**a**) Differences in mRNA expression within the hippocampus of 29 subjects with schizophrenia and 59 healthy control subjects and within the DLPFC of a largely overlapping set of 31 subjects with schizophrenia and 69 healthy control subjects. Expression values are normalized fold differences versus the mean of healthy controls. *P* values represent main effect of diagnosis in the final regression model. (**b**) Association of M30 risk genotype (T carriers) with *KCNH2*-3.1 expression within the hippocampus (data from **a**) with respect to diagnosis. All error bars represent s.e.m.

(**Fig. 3**). Using quantitative RT-PCR, we found expression of full-length *KCNH2* (1A) to be significantly lower in both the DLPFC ($P = 0.016$; **Fig. 3a**) and hippocampus ($P = 0.003$; **Fig. 3a**) of individuals with schizophrenia. Because most patients with schizophrenia receive antipsychotic drugs, which bind KCNH2 (ref. 38), some expression differences may be medication artifacts. We therefore measured *KCNH2* expression within the frontal cortex of rats after 28 d of treatment with clozapine or haloperidol across a range of doses and did not find significant medication effects (**Supplementary Fig. 1** online).

To explore the possibility that the molecular mechanism of the clinical associations involves transcriptional regulation, we tested for genotype effects on expression of *KCNH2*-1A. No significant effects were observed (for example, for M30 $P = 0.516$; **Supplementary Data 5** online). Expression of *KCNH2*-1B, a minor isoform expressed within the brain[25], did not show significant differences between control subjects and individuals with schizophrenia, nor was it significantly associated with risk genotypes (data not shown). *NOS3* expression also showed no association with these risk SNPs (for M30 $P = 0.90$; **Supplementary Data 5** and **Supplementary Note** online). These data suggest that the molecular effects of genetic risk do not affect the expression of *KCNH2*-1A or *KCNH2*-1B and may instead relate to more complicated aspects of gene processing, such as the splicing of transcripts or the expression of other isoforms.

## Identification of a brain-specific *KCNH2* isoform in humans

Using rapid amplification of 5′ complementary DNA ends (5′-RACE) on RNA pooled from the DLPFC of ten subjects with schizophrenia and beginning from exon 4 of the full-length transcript (*KCNH2*-1A; NM_000238) we identified a previously undescribed 5′ extension of exon 3 producing an isoform that originates upstream of exon 3 (**Fig. 1** and **Supplementary Data 1** and **6** online). Further cloning from a human complementary DNA library revealed that the isoform is expressed endogenously and contains all of the downstream exons of the full-length gene (through exon 15 of *KCNH2*-1A; **Fig. 4a** and **Supplementary Data 7** online). *In silico* prediction of the longest open reading frame of *KCNH2*-3.1 suggests that the majority of the 5′ extension of exon 3 would be untranslated and that the first methionine is in frame with the conserved portion of *KCNH2*-1A (**Supplementary Data 7**). As such, *KCNH2*-3.1 is expected to be missing the first 102 amino acids of *KCNH2*-1A, replacing them with six amino acids unique to this isoform. The translation of *KCNH2*-3.1 and the predicted difference in protein size was confirmed by western blot analysis of transfected HEK cells (**Fig. 4b**). Western blot analysis of human hippocampus and frontal cortex revealed a protein band of similar molecular weight to that in transfected HEK cells (**Fig. 4b**). Furthermore, neuroblastoma cells transfected with constructs encoding either or both *KCNH2*-1A or *KCNH2*-3.1 show overlapping expression of the protein isoforms on the plasma membrane (**Fig. 4c**).

To assess the potential organ selectivity of *KCNH2*-3.1, we measured the ratio of *KCNH2*-3.1 to *KCNH2*-1A mRNA levels across several tissues, including heart and three different brain regions, by quantitative RT-PCR. We found that the two forms are comparable in their expression within several brain regions (**Supplementary Data 6**), but *KCNH2*-3.1 was over three orders of magnitude less abundant than *KCNH2*-1A within the heart, suggesting a brain-specific role of *KCNH2*-3.1. As ERG family genes are moderately conserved in sequence across several species[39], we expected *KCNH2*-3.1 to be present within other mammals. By 5′-RACE, we were unable to detect *KCNH2*-3.1 homologs in mouse brain (data not shown). Moreover, *in silico* analysis revealed that the 1.1-Kb region unique to *KCNH2*-3.1 was highly degenerate outside of primates (**Supplementary Data 7**). Protein expression of *KCNH2*-3.1 was undetectable in mouse brain but was abundant within rhesus monkey DLPFC (**Fig. 4b**).

As neuronal gene expression is tightly regulated and carefully orchestrated during development, we measured the expression profiles of *KCNH2*-1A and *KCNH2*-3.1 throughout brain development in the prefrontal cortices of 283 subjects, including 39 prenatal samples (14–20 weeks of gestation) (see **Supplementary Fig. 2** and **Supplementary Data 8** and **9** online for sample information). Isoform expression patterns were similar throughout postnatal life, but we observed marked differences in their relative expression prenatally (**Supplementary Fig. 2**). *KCNH2*-3.1 transcript levels are markedly increased prenatally relative to adult levels but then decrease and stabilize shortly after birth (**Supplementary Fig. 2**). In contrast, *KCNH2*-1A expression increases throughout prenatal development until it reaches a maximum level that is sustained throughout postnatal life (**Supplementary Fig. 2**). Although these data offer only a qualitative snapshot of developmental expression patterns, they suggest differential regulation of these isoforms during early brain development and a specific role for *KCNH2*-3.1 during these early stages.

## Risk genotypes and diagnosis predict *KCNH2*-3.1 mRNA changes

*KCNH2*-3.1 mRNA expression was significantly increased within the hippocampal formation of subjects with schizophrenia versus healthy control subjects ($P = 0.012$, **Fig. 3a**). Moreover, the ratio of *KCNH2*-3.1 to *KCNH2*-1A was 2.5-fold higher in individuals with schizophrenia ($P = 0.0010$). This ratio may reflect how isoforms and homologs of *KCNH2* assemble to create heteromeric potassium channels with unique electrophysiological properties[25,40]. Additionally, higher levels of *KCNH2*-3.1 mRNA were significantly associated with risk alleles at SNPS M30, M31 and M33, even within healthy control

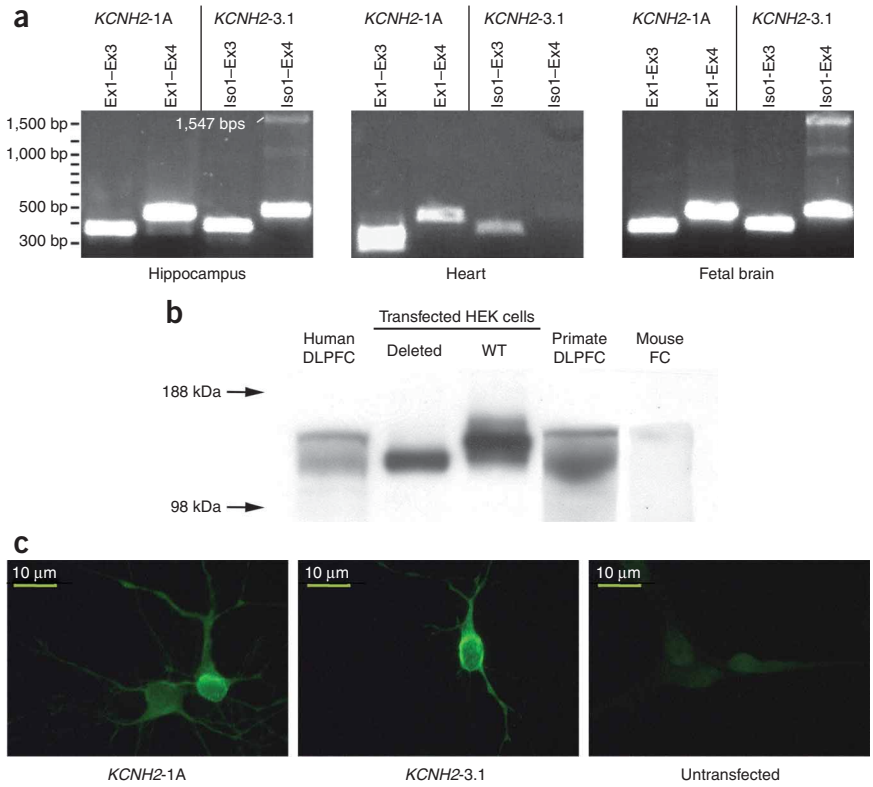


**Figure 4** Detection and quantification of *KCNH2*-3.1 mRNA and protein. (**a**) Gel with PCR products of *KCNH2*-1A and *KCNH2*-3.1 using isoform-specific primer pairs in human heart, hippocampus and fetal brain tissue extracts. PCR products for *KCNH2*-1A correspond to 373 base pairs (bp) and 463 bp, lanes 1 and 2, respectively, and for *KCNH2*-3.1 at 388 bp and 478 bp, lanes 3 and 4, respectively. The band at ~1.5 kb in Iso1-Ex4 lanes corresponds to small amounts of unspliced RNA or genomic DNA contaminant present in the samples (lane 4). (**b**) Protein expression of KCNH2-1A and KCNH2-3.1 in human, primate and mouse frontal cortex. Positive control lanes include HEK cells transfected with full-length KCNH2-1A (WT) and KCNH2-3.1. Proteins extracted from human brain regions show two distinct bands, one equivalent in size to that found in KCNH2-3.1–transfected HEK cells. However, the larger protein band observed in human brain did not correspond to the size of *KCNH2*-1A–transfected HEK proteins. Instead, the larger band occurs at ~160 kDa, which is the reported size of *KCNH2*-1A from *in vivo* protein extracts, suggesting post-translational modifications. (**c**) Primary rat neurons transfected with *KCNH2*-1A or *KCNH2*-1A–containing vectors.



subjects (**Fig. 3b**). Specifically, diagnosis and M30 genotype each had independent significant effects on *KCNH2*-3.1 expression ($P = 0.006$ and 0.002, respectively) as well as a significant interaction on expression ($P = 0.028$; **Fig. 3b**), suggesting that although risk alleles are associated with increased expression of *KCNH2*-3.1 regardless of subject group, the effect is more pronounced in subjects with schizophrenia (**Fig. 3b**). We observed this trend irrespective of ethnicity, reducing the potential confounder of genetic background (**Supplementary Data 5**). We found similar results with M31 and M33, although interactions with diagnosis were not significant (data not shown). These data support the hypothesis that the mechanism by which the disease-associated SNPs contribute to risk for schizophrenia and related phenotypes involves the regulation of *KCNH2*-3.1 transcription and further suggest that overexpression of this isoform would result in physiological effects related to the pathogenesis of the disorder.

### Functional role of KCNH2-3.1 revealed by electrophysiology

KCNH2, (also known as hERG1), a member of the tetrameric ERG-related family of potassium channels[39], is best known for its role in slow repolarization during the myocardial action potential, thereby regulating the QT interval[41]. Its distinct physiological features, namely slow activation, fast inactivation and slow and voltage-dependent deactivation[39,40,42], make KCNH2 an excellent candidate for controlling neuronal firing patterns and cortical network oscillation[43–45]. Modeling work predicts that KCNH2 is crucial for spike-frequency adaptation, or a gradual termination of a train of evoked action potentials, a common firing pattern seen in excitatory neurons in the brain[46]. Several studies have shown that inhibition of KCNH2 converts low-frequency, adapting to high-frequency, non-adapting neuronal discharges[46,47], a firing pattern necessary for sustained neuronal activity subserving numerous complex cognitive functions[48].

The slow deactivation of the KCNH2 channel is mediated by a PYP-like sensor domain (amino acids 25–136) of the KCNH2-1A amino terminus[42], most of which is missing in KCNH2-3.1 (**Fig. 5a**). We performed whole-cell recording on HEK cells transfected with either KCNH2-1A or KCNH2-3.1. When depolarized from –60 mV to various membrane potentials, KCNH2-3.1 was activated faster than KCNH2-1A (**Fig. 5b,** and **Supplementary Fig. 3** online).

When the membrane potential was hyperpolarized to −120 mV after depolarization, the *KCNH2*-1A–expressing cells showed a large, slowly deactivating 'tail current', which is completely blocked by the hERG-specific inhibitor E-4031 (ref. 49) (**Fig. 5c**), suggesting that this current is mediated solely by hERG channels. In contrast, cells transfected with *KCNH2*-3.1 showed a markedly lower tail current (**Fig. 5c**), which was also blocked by E-4031. The peak current density-voltage relationship (I-V curve) showed a substantial reduction in the peak amplitudes, particularly when cells were more substantially depolarized initially (**Supplementary Fig. 3**). In a conductance-voltage plot, KCNH2-3.1 showed a slight, but significantly reduced, steady-state tail current activation (**Fig. 5d**; V1/2: KCNH2-1A = −16.37 ± 2.55 mV; KCNH2-3.1 = −6.54 ± 4.04 mV, $P < 0.05$).

When the cells were first depolarized and held at +60 mV and then hyperpolarized at various potentials (**Fig. 5e**), the inward currents mediated by KCNH2-3.1 decayed toward baseline much faster than those mediated by KCNH2-1A (**Fig. 5e**). The deactivation phase of the KCNH2-1A currents was best fitted by a double-exponential curve, generating a slow and a fast deactivation constant ($\tau 1$ and $\tau 2$), whereas that of KCNH2-3.1 could be fitted only by a single-exponential curve, with a much slower $\tau 1$ at all repolarizing voltages tested (**Fig. 5f**). Thus, KCNH2-3.1 mediates an inward rectified $K^+$ current with markedly faster deactivation kinetics. Furthermore, when KCNH2-1A was coexpressed with KCNH2-3.1, the deactivation phase of the tail currents could be fitted by a double-exponential curve, with $\tau 1$ and $\tau 2$ that were both significantly lower than those in cells expressing

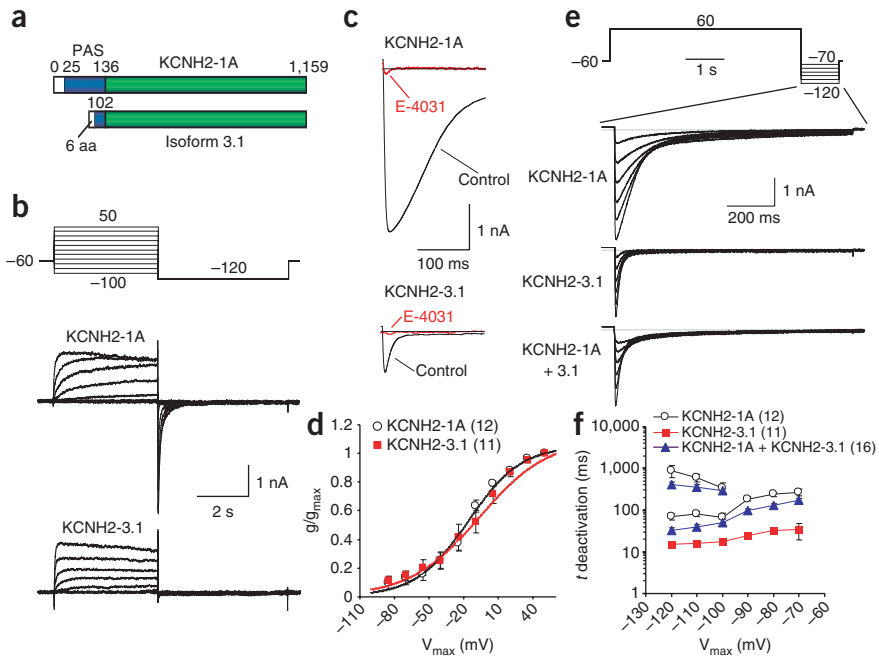


**Figure 5** Characterization of KCNH2 currents in HEK293T cells expressing KCNH2-1A and KCNH2-3.1. (**a**) Schematic diagram of KCNH2-1A and KCNH2-3.1 domain structures. Blue box, PYP-like sensor (PAS) domain. Green box, conserved amino acid sequences between isoforms. Numbers correspond to amino acid positions. (**b**) Currents evoked by voltage steps (4 s) from resting voltage ($V_H$) of −60 mV to potentials from −100 mV to +50 mV in 10-mV increments, followed by a voltage pulse to −120 mV (5 s). Top, voltage protocol. Middle and bottom: traces (corrected for leak currents) recorded from cells transfected with *KCNH2*-1A (middle) and *KCNH2*-3.1 (bottom) cDNAs. (**c**) Effects of E-4031 on tail currents evoked by a test pulse to −120 mV from holding potential of +50 mV, using the same protocol as in **b**. Traces recorded from the same cells before (black) and after (red) treatment with 10 μM E-4031 are superimposed. Top and bottom graphs show KCNH2 currents recorded from cells transfected with *KCNH2*-1A and *KCNH2*-3.1 cDNAs, respectively. (**d**) Steady-state activation curves of KCNH2-1A and KCNH2-3.1 tail currents, which were induced by the protocol shown in **b**. Numbers in parentheses indicate the number of cells recorded. $g/g_{max}$, conductance/maximum conductance ratio. (**e**) Tail currents evoked by voltage steps from +60 mV to potentials between −120 mV and −70 mV in 10-mV increments. Traces in top, middle and bottom graphs represent tail currents of cells transfected with *KCNH2*-1A, *KCNH2*-3.1 and both *KCNH2*-1A and *KCNH2*-3.1, respectively. (**f**) Semilogarithmic plot of deactivation time constants of KCNH2-1A and KCNH2-3.1 currents at various repolarizing voltages. Top plot (between −210 mV and −100 mV) corresponds to τ2 for HEK cells transfected with *KCNH2*-1A alone or cotransfected with *KCNH2*-1A and *KCNH2*-3.1, whereas the bottom plots correspond to τ1 for all transfection combinations. Data are means ± s.e.m.

KCNH2-1A alone (**Fig. 5f**; analysis of variance, $P < 0.05$), suggesting codominant channel behavior intermediate to each channel.

We next examined the functional role of KCNH2-3.1 in cortical neurons. Given that rodent central nervous system neurons express *KCNH2*-1A, but not *KCNH2*-3.1, KCNH2-3.1 introduced into these neurons would presumably form complexes with the endogenous KCNH2-1A, thereby changing the deactivation kinetics of the $K^+$ current. In rat primary cortical neurons transfected with a GFP marker alone, application of a voltage protocol similar to that in **Figure 5e** elicited a series of tail currents that were blocked by E-4031 (**Fig. 6a**). Subtraction of the currents after E-4031 treatment from control currents generated pure KCNH2-1A–mediated current that showed typical, slow deactivation kinetics (**Fig. 6a**). In contrast, application of the same protocol to neurons transfected with KCNH2-3.1 (plus GFP marker) elicited a considerably reduced tail current with significantly faster deactivation (**Fig. 6a**). At −100 mV, the introduction of KCNH2-3.1 reduced the τ2 (initial fast component) and τ1 (slow component) of tail currents by 83% and 92%, respectively (**Fig. 6b**). Transfection of human *KCNH2*-1A into rat cortical neurons resulted in tail currents very similar to those of untransfected or GFP-transfected neurons (**Supplementary Fig. 3**), further supporting that KCNH2-1A and KCNH2-3.1 have very different deactivation kinetics.

To test whether endogenous KCNH2-1A and exogenous KCNH2-3.1 form a functional complex, we examined action potentials induced by a step depolarization under the current-clamp conditions. In neurons transfected with *KCNH2*-3.1, a 1-s depolarization induced significantly more spikes compared with control (untransfected) and GFP-transfected neurons (**Fig. 6c**). A systematic analysis showed a general increase in spike frequencies in *KCNH2*-3.1–expressing neurons injected with more than 30 pA depolarizing current (**Fig. 6d,e**). E-4031 significantly increased firing frequency, even in neurons expressing *KCNH2*-3.1 (**Fig. 6f**). Again, the firing behavior of rat neurons expressing human *KCNH2*-1A was very similar to that of control neurons (**Supplementary Fig. 3c,d**).

In addition to increasing firing frequency, expression of *KCNH2*-3.1 seemed to change the firing pattern from a typical, adapting pattern to a nonadapting pattern (**Fig. 6c**). To better quantify this change, we measured instantaneous frequency (inverse of the first inter-pulse interval versus spike number). Indeed, both control and GFP- expressing neurons exhibited a gradual decline of instantaneous frequency, whereas instantaneous frequency remained stable during the entire course of depolarization in *KCNH2*-3.1–expressing neurons (**Fig. 6e**). Taken together, these results suggest that expression of *KCNH2*-3.1 in human prefrontal cortex significantly increases neuronal excitability and offers a potential mechanism for persistent or overactive neuronal discharges observed in neurons of the prefrontal cortex during working memory tasks[48].

## DISCUSSION

We report a previously undescribed genetic association with schizophrenia within a small region of intron 2 of *KCNH2*, which was observed in a meta-analysis of five independent clinical data sets. Our results also suggest that the molecular mechanism of genetic susceptibility relates to changes in gene expression and regulation of an isoform of *KCNH2* with unique physiologic properties. The sequence of hypothesis-driven experiments and tests leading to this convergent evidence, from initial genetic screening to genetic association with aspects of human hippocampal structure and hippocampal and DLPFC function and gene expression to confirmatory experiments in tissue culture is summarized in **Supplementary Figure 4** online. Although we report here the significant association of several SNPs across independent samples and by meta-analysis, the exact risk structure may vary between populations, whereas the regional location

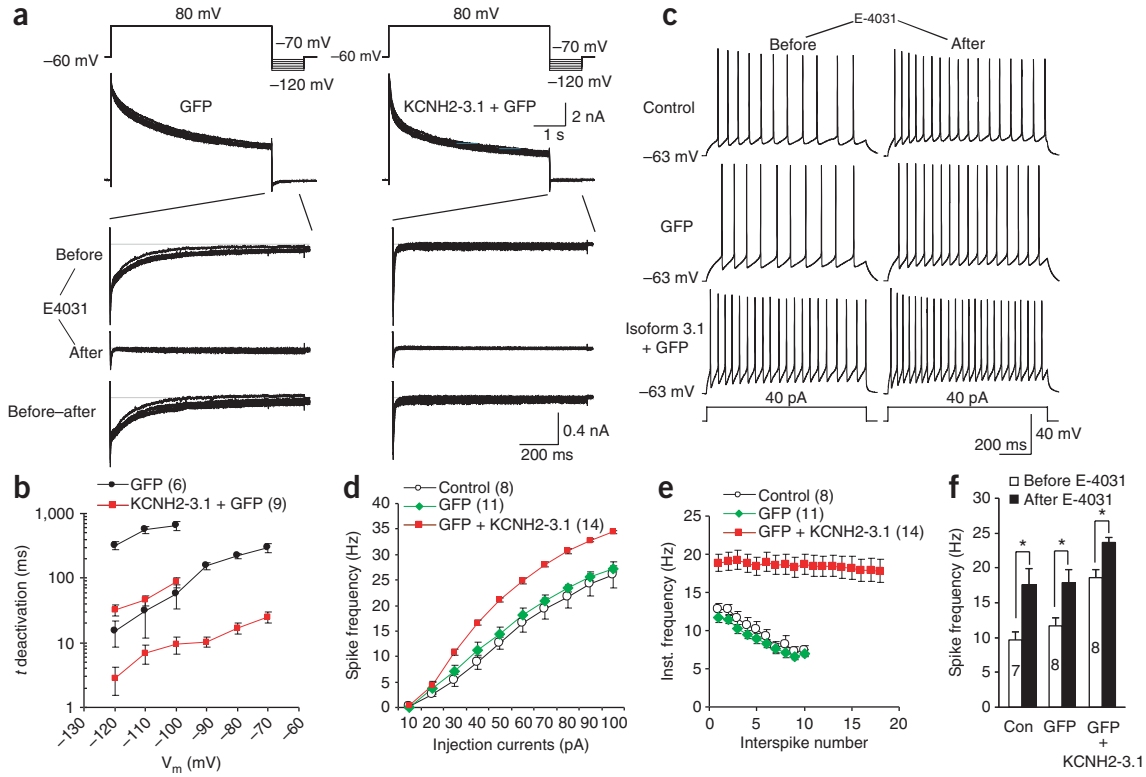


**Figure 6** Effect of KCNH2-3.1 on repolarization-induced tail currents and firing patterns in cortical neurons. (**a**) KCNH2-mediated tail currents in GFP- (left) and *KCNH2*-3.1–transfected (right) neurons before and after application of E4031. Top plot diagrams the voltage protocol. Bottom plot represents E-4031–sensitive current (that is, hERG current) generated by subtracting the before inhibitor and after inhibitor currents. (**b**) Semilogarithmic plot of deactivation time constants of E-4031–sensitive currents at various repolarizing voltages in transfected primary cortical neurons. The −120 mV to −100 mV decay of E-4031–sensitive currents was fitted by double-exponential functions (bottom curves: τ1, top curves: τ2), whereas the −90 mV to −70 mV time course followed single-exponential functions (τ). (**c**) Effect of *KCNH2*-3.1 overexpression in rat cortical neurons on action potential discharge evoked by long depolarizing pulse (40 pA, 1 s) before (left) and after (right) application of E-4031. (**d**) Spike frequencies (number of spikes per second) versus applied depolarizing currents in transfected primary cortical neurons. (**e**) Effect of KCNH2-3.1 on spike frequency adaptation, depicted as instantaneous frequency (inverse of interpulse interval) versus the corresponding spikes interval evoked by a 4-pA depolarizing pulse. (**f**) Effect of E-4031 on repetitive action potential discharge of transfected cortical neurons. Data are means ± s.e.m. $^*P < 0.01$.



and overall effect on *KCNH2* gene processing may remain consistent with what is described here. The splicing mechanism related to variation in this region of *KCNH2* is yet to be determined (see **Supplementary Note**).

To our knowledge, the region of interest on chromosome 7q36.1 has not, to date, been reported as a major locus in the few genome-wide association studies of psychiatric illnesses[50,51]. These negative results may reflect the fact that such psychiatric genome-wide association studies have relied largely on Affymetrix 5.0 SNP arrays, whose coverage is notably lacking over this genomic region. Conversely, the *P* values reported here would not be significant if we corrected for all SNPs in the genome. Scanning the genome with hundreds of thousands of SNPs and employing the necessary rigid statistical correction because of no prior probability of any SNP being positive is a popular strategy at the moment, as it makes no assumptions about biology or function. This strategy has the appeal of a level of statistical significance being clear and incontrovertible. However, statistical significance does not, in and of itself, imply biological significance, nor does it necessarily identify the genes most likely to be important in unraveling new strategies for prevention and treatment.

To move beyond statistical association with clinical diagnosis and to obtain convergent evidence for association between *KCNH2* and schizophrenia-related biology, we have performed a series of convergent experiments testing risk-associated SNPs on several intermediate biological phenotypes (**Supplementary Fig. 4**). Although we believe our deductive, hypothesis-driven strategy minimizes serendipity, it does involve a number of tests. Thus, the potential for spurious association because of multiple testing is necessary to consider. Three of the four SNPs showing association in a meta-analysis of five independent clinical data sets were tested for association with biological phenotypes related to risk for schizophrenia and to molecular processing of *KCNH2* transcripts. A consistent pattern of allelic association, involving cognition and structural and functional imaging, was found in normal subjects and in expression of the 3.1 isoform in brain tissue from individuals with schizophrenia and controls of various ethnic backgrounds. The likelihood that by chance the same risk-associated alleles would predict variation in each of these independent phenotypes across these diverse samples and always in the direction of abnormality associated with illness is remote.

Exploration of the potential electrophysiological effects of elevated *KCNH2*-3.1 levels on neuronal repolarization and spike frequency has noteworthy implications for both normal cortical function and the pathophysiology of psychosis. Cortical information processing is dependent on well orchestrated, persistent neuronal firing within cortical circuits[45]. For example, neurons in the prefrontal cortex show sustained firing of high-frequency activity during the delay

period that is thought to be crucial for working memory[48]. The cellular mechanism for this sustained firing is not clear. We found that expression of *KCNH2*-3.1 in cultured cortical neurons results in a much faster deactivation of the hERG channels, leading to a marked increase in spike frequency and a conversion from adapting to predominantly nonadapting firing patterns. Such sustained firing patterns may be important for higher-order cognition and suggest a role for the primate-specific *KCNH2*-3.1 in normal human cognitive processing. However, this key evolutionary change in activation kinetics may require specific titration of isoform abundances to achieve optimum signal-to-noise relationships. The 2.5-fold higher relative *KCNH2*-3.1 expression in the schizophrenic brain might imbalance this titration, resulting in abnormally increased neuronal excitability and disruption of neuronal firing patterns and regulation of signal-to-noise ratios[12].

The discovery of *KCNH2*-3.1 may also have therapeutic implications. Some typical and atypical antipsychotic drugs bind and inhibit *KCNH2* with affinities comparable to their affinities for dopamine D2 receptors[38]. Whereas D2 receptor affinity is thought to account for the therapeutic effects of antipsychotics, KCNH2 binding is responsible at least for side effects such as altered QT interval[38] or even sudden cardiac failure[52]. Given that KCNH2 controls neuronal excitability and firing patterns, could the therapeutic effects of antipsychotic drugs also be related to their affinities for the brain-specific isoforms of KCNH2? Although the binding properties of antipsychotic drugs to KCNH2-3.1 remain to be tested, the unique structure of KCNH2-3.1, its role in nonadaptive firing, its low expression in heart and its elevated expression in brains of individuals with schizophrenia and genetic risk carriers make it reasonable to speculate that selective inhibition of KCNH2-3.1, but not of KCNH2-1A, would improve the disorganized firing in schizophrenia brain without eliciting cardiac side effects.

In conclusion, we have identified and characterized a previously undescribed, primate-specific, brain-enriched potassium channel with a potential genetic association with risk for schizophrenia. Healthy control carriers of risk alleles show a schizophrenia-like shift in cognitive traits (IQ and processing speed), hippocampal volume and physiological engagement during memory processing, and in prefrontal physiologic engagement during executive cognition. The mechanism of these associations seems to be related to genetic regulation of *KCNH2*-3.1, which has unique electrophysiological properties and expressional dependence on risk-associated genotypes. Together, these results may provide new insight into the etiology of schizophrenia and a fresh direction for therapeutic discovery.

## METHODS

**Genetic association cohorts.** We included five independent clinical data sets in this study; two family-based cohorts of European ancestry (367 families) and three case control cohorts also of European ancestry (1,158 cases, 1,704 controls) (see **Supplementary Methods** online for details). We took postmortem brain from the CBDB Postmortem Brain Collection and Life Span Series consisting of tissue from 31 subjects with schizophrenia, 69 control subjects, 39 fetal samples and an additional 244 control subjects covering a range of ages (**Supplementary Methods and Supplementary Data 8** online). All research subjects gave written informed consent under a protocol approved by the human subjects research committees of the appropriate institution (see **Supplementary Methods**) and by the Combined Neuroscience Institutional Review Board of the US National Insistutes of Health (NIH) intramural research program.

**Candidate gene screening.** We selected 10 candidate genes from those previously reported as differentially expressed between individuals with schizophrenia and healthy controls[16]. We genotyped SNPs tagging haplotype blocks determined from HapMap Caucasian European (CEU) population (release 15) and overlapping with part or all of the genes of interest on a screening subsample of 175 families (698 subjects of European descent) from the CBDB family dataset. We genotyped all SNPs with 5-exonuclease TaqMan assays as previously described[53]. We tested haplotype association with the FBAT[17], evaluated at $\alpha = 0.05$ using simulation with 1,000 iterations and subjected to Bonferroni correction.

***KCNH2* genotyping and resequencing.** We genotyped 43 SNPs within a 65.2-kb region of *KCNH2* and *NOS3* (chromosome 7 bases 150,280,464–150,345,679). We resequenced a total of 13.5 kb in 48 subjects with schizophrenia, including 10.4 kb flanking rs1036145 (chromosome 7 bases 150,299,575–150,309,948) and 3.1 kb upstream of exon 3 (chromosome 7 bases 150,287,750–150,290,865) with high cross-species conservation in the University of California at Santa Cruz genomes database (http://genome.ucsc.edu/). Resequencing found 11 previously undescribed SNPs and no coding polymorphisms (details in **Supplementary Methods**).

**Cognitive testing.** Depending on the cognitive test, data were available for between 230 and 330 normal individuals not part of the clinical association data sets. All subjects gave written informed consent under a protocol approved by the Combined Neuroscience Institutional Review Board of the NIH. The tests included tasks aimed at assessing a wide range of cognitive features significantly affected in subjects with schizophrenia and in their unaffected siblings[12–15]. Factor analysis of 24 performance scores identified seven factors that explained 68% of the variance on these measures[28]. We used these seven factors to assess genotype effects on cognitive task performance (see below) and labeled them as follows: verbal memory, N-back, visual memory, processing speed and IQ, card sorting, attention and digit span. Further information regarding the test measures included in each factor is provided in **Supplementary Data 3**.

**Statistical genetics analysis.** We analyzed SNP association within families by FBAT[17] and by logistic regression in unrelated cases and controls (**Supplementary Methods**). We performed meta-analyses with the R package Catmap[20] based on fixed-effects estimates where the heterogeneity (Q statistic) of genetic effects was not significant at $\alpha = 0.05$ (markers M17, M19, M30, M31 and M33) and random-effects estimates (markers M16 and M20) where significant differences in genetic effects were found across samples (**Supplementary Methods**).

We tested genotype effects on cognitive intermediate phenotypes in control subjects using linear regression, adjusting for age and gender. We used permutation testing based on 1,000 replicates to examine the pattern of associations of SNPs M30, M31 and M33 with the cognitive factor scores to assess the likelihood that for each SNP the schizophrenia risk-associated allele would be associated with relatively poorer performance on the same factor.

**Quantitative real-time PCR.** Details about the collection, screening and dissection processes for human brain tissue have been previously described[54], and demographic statistics about the brain specimens used here are provided in the **Supplementary Methods**. We measured gene expression by quantitative real-time RT-PCR. We designed probes to differentiate between *KCNH2* isoforms through hybridizing to isoform-specific exons (**Supplementary Methods**).

**Antipsychotic drug effects in rats.** Briefly, we measured *KCNH2* mRNA in the frontal cortex of male Sprague-Dawley rats (weight 250 g) treated chronically (for 28 d) with clozapine (0.5, 5 or 10 mg per kg body weight) and haloperidol (0.08, 0.6 or 2 mg per kg body weight) using Taqman ABI assay Rn00588515_m1. The expression data of a target gene were normalized to a geometric mean of three control genes. Further details are provided in the **Supplementary Methods**.

**Custom Illumina microarray analysis of fetal tissues.** Microarray chips were generated in the National Human Genome Research Institute Microarray Core Facility from 44,544 70-mer probes obtained from the Illumina Oligoset HEEBO (http://www.microarray.org/sfgf/heebo.do). We amplified RNA samples from the lifespan DLPFC collection (500 ng) and labeled them with fluorescent dye (Cy5)(GE Healthcare). We hybridized each sample to

microarrays simultaneously with a reference standard (labeled with Cy3) consisting of a pool of RNA from many brain tissue samples. Analysis was done with limma R package[55].

**Imaging methods.** All imaging subjects were healthy volunteers of European descent (not part of the clinical association data) without significant differences in age, gender, IQ score or education across genotype groups (**Supplementary Data 4** contains demographic information). All subjects gave written informed consent under a protocol approved by the Combined Neuroscience Institutional Review Board of the NIH. All analyses were done in SPM (Statistical Parametric Mapping, http://www.fil.ion.ucl.ac.uk/spm) with SNPs effects assessed with random effects analyses. For gray matter volumes, we performed optimized voxel-based morphometry following standardized methods with appropriate covariates as described previously[22–24] (**Supplementary Methods**) ($n = 141$).

During 3T blood oxygen level–dependent (BOLD) fMRI scanning described previously[30], normal subjects performed a declarative memory task ($n = 79$) and an executive working memory task (N-back, $n = 178$) to robustly engage the hippocampal formation[30] and dorsolateral prefrontal cortex[37], respectively (**Supplementary Methods**). We performed random-effects analyses on *a priori*–defined regions of interest with genotype as a predictor (**Supplementary Methods**). We used FDR corrections ($\alpha = 0.05$) to control for the expected proportion of false positives among suprathreshold voxels.

**Isoform 3.1 cloning and expression.** We performed 5′-RACE with a 5′-RACE System (v2.0) as recommended by the manufacturer (Invitrogen). We made template from commercially available total RNA from ten human cell lines and tissues (Stratagene; **Supplementary Methods**). We cloned isoform3.1 cDNA by long PCR with specific primers and high-fidelity DNA polymerase into vector pZero-Blunt (Invitrogen) and then subcloned it into vector pcDNA3 (Invitrogen). We transfected HEK293 cells (American Type Culture Collection) with the *KCNH2*-1A vector, *KCNH2*-3.1 vector, or empty vector using standard methods. We measured protein expression by western blotting and immunocytochemistry using standard techniques as described in the **Supplementary Methods**.

**Electrophysiology.** We cultured HEK293T (American Type Culture Collection) cells and primary cortical neurons were and transfected them by nucleofection, as previously described[56]. We identified transfected cells by GFP expression under fluorescence microscopy, and we performed whole-cell recordings as detailed in the **Supplementary Methods**. We obtained tail currents during 4-s voltage steps shown in the upper panels of **Figures 5b**, **5e and 6a**, and we fitted them by exponential functions and analyzed them in detail as detailed in the **Supplementary Methods**. We also assessed transfected cortical neurons for repetitive firing properties using a long depolarizing pulse (40 pA, 1 s) as described in the **Supplementary Methods.**

**Accession codes.** The sequence for *KCNH2*-3.1 has been deposited in GenBank with accession number FJ938021.

*Note: Supplementary information is available on the Nature Medicine website.*

ACKNOWLEDGMENTS

We thank J. Hardy, J. Duckworth and P. Momeni for technical assistance with high G-C content sequencing. We also thank J. Hardy, D. Goldman, A. Law and W. Chen for their very helpful review of the manuscript. We thank R. Straub and M. Mayhew for their input on statistical genetics analysis, M. Barenboim for help with bioinformatics and M. Herman and S. Mitkus for their help with postmortem tissue. We are extremely grateful for the assistance of G. Liu and S. Chen in the cloning and sequencing of *KCNH2*-3.1. We also would like to thank H.-J. Möller, P. Muglia and coworkers at the Department of Psychiatry, Ludwig Maximilians University for their help with subject recruitment and evaluation. S.J. Huffaker was partially supported by the US National Institutes of Health/Cambridge University Health Science Scholars and Medical Scientist Training Programs. Recruitment of the individuals with schizophrenia at Ludwig Maximilians University was supported by GlaxoSmithKline. Human fetal tissue was obtained from the NICHD Brain and Tissue Bank for Developmental Disorders at the University of Maryland.

AUTHOR CONTRIBUTIONS

S.J.H. designed the study, collected and analyzed the data and wrote the paper; D.R.W. designed the study, analyzed data and wrote the paper; K.K.N. performed the statistical genetics and wrote the paper; J. Chen, Y.J. and J.S. performed western blot and HEK expression experiments; F.S., V.M., J.H.C., M.J.P. and A.M.-L. performed the imaging experiments and edited the paper; F.Y., B.K.L. and J. Chang performed the electrophysiology experiments; D.R. and I.G. collected the German cohort samples; A.S. and K.M. collected the Armenian cohort samples; A.B. and G.C. collected the Italian data set; B.L., J.E.K. and T.M.H. collected the postmortem cohort samples; D.R.W., J.E.K., M.F.E., T.E.G., T.M.H., V.M. and J.H.C. collected the CBDB cohort samples.

Published online at http://www.nature.com/naturemedicine/
Reprints and permissions information is available online at http://npg.nature.com/reprintsandpermissions/

1. Ioannidis, J.P., Ntzani, E.E., Trikalinos, T.A. & Contopoulos-Ioannidis, D.G. Replication validity of genetic association studies. *Nat. Genet.* **29**, 306–309 (2001).
2. Trikalinos, T.A., Ntzani, E.E., Contopoulos-Ioannidis, D.G. & Ioannidis, J.P. Establishment of genetic associations for complex diseases is independent of early study findings. *Eur. J. Hum. Genet.* **12**, 762–769 (2004).
3. Weiss, K.M. & Terwilliger, J.D. How many diseases does it take to map a gene with SNPs? *Nat. Genet.* **26**, 151–157 (2000).
4. Frayling, T.M. *et al.* A common variant in the *FTO* gene is associated with body mass index and predisposes to childhood and adult obesity. *Science* **316**, 889–894 (2007).
5. Grarup, N. *et al.* Studies of association of variants near the *HHEX*, *CDKN2A/B*, and *IGF2BP2* genes with type 2 diabetes and impaired insulin release in 10,705 Danish subjects: validation and extension of genome-wide association studies. *Diabetes* **56**, 3105–3111 (2007).
6. Callicott, J.H. *et al.* Abnormal fMRI response of the dorsolateral prefrontal cortex in cognitively intact siblings of patients with schizophrenia. *Am. J. Psychiatry* **160**, 709–719 (2003).
7. Cannon, T.D. *et al.* The inheritance of neuropsychological dysfunction in twins discordant for schizophrenia. *Am. J. Hum. Genet.* **67**, 369–382 (2000).
8. Egan, M.F. *et al.* Relative risk of attention deficits in siblings of patients with schizophrenia. *Am. J. Psychiatry* **157**, 1309–1316 (2000).
9. Egan, M.F. *et al.* Relative risk for cognitive impairments in siblings of patients with schizophrenia. *Biol. Psychiatry* **50**, 98–107 (2001).
10. Honea, R.A. *et al.* Is gray matter volume an intermediate phenotype for schizophrenia? A voxel-based morphometry study of patients with schizophrenia and their healthy siblings. *Biol. Psychiatry* **63**, 465–474 (2008).
11. Winterer, G. *et al.* Prefrontal broadband noise, working memory and genetic risk for schizophrenia. *Am. J. Psychiatry* **161**, 490–500 (2004).
12. Winterer, G. & Weinberger, D.R. Genes, dopamine and cortical signal-to-noise ratio in schizophrenia. *Trends Neurosci.* **27**, 683–690 (2004).
13. Straub, R.E. & Weinberger, D.R. Schizophrenia genes—famine to feast. *Biol. Psychiatry* **60**, 81–83 (2006).
14. Peirce, T.R. *et al.* Convergent evidence for 2′,3′-cyclic nucleotide 3′-phosphodiesterase as a possible susceptibility gene for schizophrenia. *Arch. Gen. Psychiatry* **63**, 18–24 (2006).
15. Talkowski, M.E., Chowdari, K., Lewis, D.A. & Nimgaonkar, V.L. Can RGS4 polymorphisms be viewed as credible risk factors for schizophrenia? A critical review of the evidence. *Schizophr. Bull.* **32**, 203–208 (2006).
16. Prabakaran, S. *et al.* Mitochondrial dysfunction in schizophrenia: evidence for compromised brain metabolism and oxidative stress. *Mol. Psychiatry.* **9**, 684–697, 643 (2004).
17. Horvath, S., Xu, X. & Laird, N.M. The family based association test method: strategies for studying general genotype-phenotype associations. *Eur. J. Hum. Genet.* **9**, 301–306 (2001).
18. The International HapMap Project. The International HapMap Project. *Nature* **426**, 789–796 (2003).
19. Cloninger, C.R. *et al.* Genome-wide search for schizophrenia susceptibility loci: the NIMH Genetics Initiative and Millennium Consortium. *Am. J. Med. Genet.* **81**, 275–281 (1998).
20. Nicodemus, K.K. Catmap: case-control and TDT meta-analysis package. *BMC Bioinformatics* **9**, 130 (2008).
21. Chanock, S.J. *et al.* Replicating genotype-phenotype associations. *Nature* **447**, 655–660 (2007).
22. Wellcome Trust Case Control Consortium. Genome-wide association study of 14,000 cases of seven common diseases and 3,000 shared controls. *Nature* **447**, 661–678 (2007).
23. Allen, N.C. *et al.* Systematic meta-analyses and field synopsis of genetic association studies in schizophrenia: the SzGene database. *Nat. Genet.* **40**, 827–834 (2008).
24. Ioannidis, J.P. *et al.* Assessment of cumulative evidence on genetic associations: interim guidelines. *Int. J. Epidemiol.* **37**, 120–132 (2008).
25. Guasti, L. *et al.* Expression pattern of the ether-a-go-go-related (ERG) family proteins in the adult mouse central nervous system: evidence for coassembly of different subunits. *J. Comp. Neurol.* **491**, 157–174 (2005).
26. Harrison, P.J. The neuropathology of schizophrenia. A critical review of the data and their interpretation. *Brain* **122**, 593–624 (1999).
27. Weinberger, D.R. *et al.* Prefrontal neurons and the genetics of schizophrenia. *Biol. Psychiatry* **50**, 825–844 (2001).
28. Genderson, M.R. *et al.* Factor analysis of neurocognitive tests in a large sample of schizophrenic probands, their siblings, and healthy controls. *Schizophr. Res.* **94**, 231–239 (2007).

29. Hariri, A.R. & Weinberger, D.R. Imaging genomics. *Br. Med. Bull.* **65**, 259–270 (2003).
30. Hariri, A.R. *et al.* Brain-derived neurotrophic factor val66met polymorphism affects human memory-related hippocampal activity and predicts memory performance. *J. Neurosci.* **23**, 6690–6694 (2003).
31. Bookheimer, S.Y. *et al.* Patterns of brain activation in people at risk for Alzheimer's disease. *N. Engl. J. Med.* **343**, 450–456 (2000).
32. Egan, G. *et al.* Neural correlates of the emergence of consciousness of thirst. *Proc. Natl. Acad. Sci. USA* **100**, 15241–15246 (2003).
33. Davachi, L. & Goldman-Rakic, P.S. Primate rhinal cortex participates in both visual recognition and working memory tasks: functional mapping with 2-DG. *J. Neurophysiol.* **85**, 2590–2601 (2001).
34. Royall, D.R. *et al.* Executive control function: a review of its promise and challenges for clinical research. A report from the Committee on Research of the American Neuropsychiatric Association. *J. Neuropsychiatry Clin. Neurosci.* **14**, 377–405 (2002).
35. Gray, J.R., Chabris, C.F. & Braver, T.S. Neural mechanisms of general fluid intelligence. *Nat. Neurosci.* **6**, 316–322 (2003).
36. Duncan, J. *et al.* A neural basis for general intelligence. *Science* **289**, 457–460 (2000).
37. Callicott, J.H. *et al.* Physiological dysfunction of the dorsolateral prefrontal cortex in schizophrenia revisited. *Cereb. Cortex* **10**, 1078–1092 (2000).
38. Kongsamut, S., Kang, J., Chen, X.L., Roehr, J. & Rampe, D. A comparison of the receptor binding and HERG channel affinities for a series of antipsychotic drugs. *Eur. J. Pharmacol.* **450**, 37–41 (2002).
39. Warmke, J.W. & Ganetzky, B. A family of potassium channel genes related to eag in *Drosophila* and mammals. *Proc. Natl. Acad. Sci. USA* **91**, 3438–3442 (1994).
40. Wimmers, S., Bauer, C.K. & Schwarz, J.R. Biophysical properties of heteromultimeric erg $K^+$ channels. *Pflugers Arch.* **445**, 423–430 (2002).
41. Sanguinetti, M.C. & Tristani-Firouzi, M. hERG potassium channels and cardiac arrhythmia. *Nature* **440**, 463–469 (2006).
42. Morais Cabral, J.H. *et al.* Crystal structure and functional analysis of the HERG potassium channel N terminus: a eukaryotic PAS domain. *Cell* **95**, 649–655 (1998).
43. Bracci, E., Vreugdenhil, M., Hack, S.P. & Jefferys, J.G. On the synchronizing mechanisms of tetanically induced hippocampal oscillations. *J. Neurosci.* **19**, 8104–8113 (1999).
44. Bazhenov, M., Timofeev, I., Steriade, M. & Sejnowski, T.J. Potassium model for slow (2–3 Hz) *in vivo* neocortical paroxysmal oscillations. *J. Neurophysiol.* **92**, 1116–1132 (2004).
45. Canolty, R.T. *et al.* High gamma power is phase-locked to theta oscillations in human neocortex. *Science* **313**, 1626–1628 (2006).
46. Chiesa, N., Rosati, B., Arcangeli, A., Olivotto, M. & Wanke, E. A novel role for HERG $K^+$ channels: spike-frequency adaptation. *J. Physiol. (Lond.)* **501**, 313–318 (1997).
47. Sacco, T., Bruno, A., Wanke, E. & Tempia, F. Functional roles of an ERG current isolated in cerebellar Purkinje neurons. *J. Neurophysiol.* **90**, 1817–1828 (2003).
48. Wang, Y. *et al.* Heterogeneity in the pyramidal network of the medial prefrontal cortex. *Nat. Neurosci.* **9**, 534–542 (2006).
49. Spector, P.S., Curran, M.E., Keating, M.T. & Sanguinetti, M.C. Class III antiarrhythmic drugs block HERG, a human cardiac delayed rectifier $K^+$ channel. Open-channel block by methanesulfonanilides. *Circ. Res.* **78**, 499–503 (1996).
50. O'Donovan, M.C. *et al.* Identification of loci associated with schizophrenia by genome-wide association and follow-up. *Nat. Genet.* **40**, 1053–1055 (2008).
51. Sullivan, P.F. *et al.* Genomewide association for schizophrenia in the CATIE study: results of stage 1. *Mol. Psychiatry* **13**, 570–584 (2008).
52. Witchel, H.J., Hancox, J.C., Nutt, D.J. & Wilson, S. Antipsychotics, HERG and sudden death. *Br. J. Psychiatry* **182**, 171–172 (2003).
53. Livak, K.J. Allelic discrimination using fluorogenic probes and the 5′ nuclease assay. *Genet. Anal.* **14**, 143–149 (1999).
54. Lipska, B.K. *et al.* Expression of Drosoph. Inf. Serv.C1 binding partners is reduced in schizophrenia and associated with Drosoph. Inf. Serv.C1 SNPs. *Hum. Mol. Genet.* **15**, 1245–1258 (2006).
55. Smyth, G.K. Linear models and empirical bayes methods for assessing differential expression in microarray experiments. *Stat. Appl. Genet. Mol. Biol.* **3**, Article3 (2004).
56. Nagappan, G. *et al.* Control of extracellular cleavage of ProBDNF by high frequency neuronal activity. *Proc. Natl. Acad. Sci. USA* **106**, 1267–1272 (2009).
57. Luna, A. & Nicodemus, K.K. snp.plotter: an R-based SNP/haplotype association and linkage disequilibrium plotting package. *Bioinformatics* **23**, 774–776 (2007).